복합 재료로 구성된 축대칭 원판에서의 열응력

Thermal Stresses in a Bimaterial Axisymmetric Disk-Approximate and Exact Solutions

정 철 섭*
Chung, Chul-Sup
김 기 석**
Kim, Ki-Seok

요 약

2가지 이상의 재질로 결합된 구조물이 온도 변화를 받으면 열응력이 발생한다. 이러한 응력은 재질간의 열팽창계수가 서로 상이하여 생긴다. 본 논문에서는 균일한 온도변화를 받는 복합 재료로 이루어진 축대칭 원판(disk)에 대한 응력상태를 구하는 공식을 유도하였다. 먼저, 재료역학원리를 이용하여 근사해를 구한 후, Eigenfunction series를 전개하여 탄성학적인 정확해(Exact Solution)를 구하였다. 또한 정확해는 유한요소법으로 구한 해와 비교하였다. 상기 근사해로는 연계면에서의 응력분포를 예측하는 데 어려움이 있었으나, 정확해는 유한요소법으로 구한 결과와 대체로 일치하고 있어 응력분포를 충분히 예측할 수 있었다. 따라서, 본 논문에서 구한 정확해(Exact Solution) 공식은 복합재료로 구성된 구조물의 연계면에서의 응력분포를 결정하는 데 유용하다.

Abstract

It is well known that structures constructed by bonding two or more materials and then subjected to temperature change experience thermal stress. This stress results from thermal expansion mismatch of materials. The present paper derives formulas for the stresses in a bimaterial axisymmetric disk which is subjected to a uniform temperature change. First, an approximate solution following strength-of-materials principles is developed. However, the strength-of-materials solution has difficulty in predicting both the peak value of interfacial stresses and its associated distribution. Next, a solution consistent with the theory of elasticity is developed by way of an eigenfunction expansion approach. The eigenfunction analysis is compared with finite element stress analysis results for a specific numerical example. Finite element analysis results show that the interfacial stresses are adequately predicted by eigenfunction solution. Therefore, the method developed in this paper will be useful in determination of the interfacial stress state.

* 건양대학교 기계공학과
** 한국원자력연구소 기계설계부 연구원

이 논문에 대한 토론을 1995년 9월 30일까지 본 학회에 보내주시면 1996년 3월호에 그 결과를 게재하겠습니다.

1. Introduction

Thermal stress analysis plays a key role in the design of bimaterial(or multilayered) structures such as silicon wafers commonly encountered in the microelectronic industry. For example, the deposition of various layers at high temperatures introduces stresses in silicon wafers. These stresses are maximum at the interface between material layers. Thermal stresses arise in-service in these structures due to the thermal expansion mismatch of materials. Because of the importance of the silicon wafer in industrial applications, the distribution of interfacial stress in a bimaterial axisymmetric disk form the main motivation of this research.

Many researchers have been concerned with developing solutions for the state of stress along the interface in a bimaterial structure. Timoshenko(1925) investigated the case of b-metal thermostates subjected to a spatially uniform temperature change. In his analysis, Timoshenko acknowledged the existence of interfacial shear and normal "edge-effect" stresses, but did not provide solutions for them. Vilms and Kerps(1981) considered a layered structure in the form of a long laminated strip with rectangular cross section which was amenable to analysis by beam theory, in which each layer of the structure possessed a unique value for modulus of elasticity, temperature, and thickness. The analysis was an extension of Timoshenko's bi-metal problem to multilayered thin films on a thick substrate, and was capable of predicting the longitudinal(bending) stress in each layer and curvature induced by the differential thermal strains. A significant limitation of the simple analyses mentioned above was the inability to predict shear and normal(peeling) stress magnitude at the material interface. Delamination/fracture along the interface cannot occur without the presence of these stress components. Hess(1969a, b) studied the stresses resulting from differential expansion in a composite, formed by bonding together two rectangular strips of different materials. His solution was obtained as a series of eigenfunctions, each of which varies exponentially along the axis of strip. Suhir(1986, 1988, 1989) recently presented the solutions for the stresses in bi-metal thermostat whch enable the investigator to approximate the shear and peeling stresses at the interface of the two metals. These previous investigations are not directly applicable to the problem of the layered disk, which is an axisymmetric structure. Previous work has dealt only with plane stress or plane strain.

The present paper presents formulas for the stress state in a bimaterial disk subjected to a uniform temperature change. The exact solution is obtained by the superposition of a strength of materials solution and a theory of elasticity solution via an eigenfunction expantion approach.

2. Problem Description

The physical configuration under investigation consists of two disks bonded together and then uniformly heated(or cooled) from T_0 to T_1, where $\Delta T = T_1 - T_0$. Fig. 1 is a schematic of the bimaterial disk system. Materials are assumed isotropic, and the physical properties(Young's modulus(E) and the coefficient of thermal expansion(α)) are assumed to have unique values in each layer. If the coefficients of thermal expansion for the two materials comprising the disk differ, the heating will cause elastic deformations and stresses to occur. The purpose of this analysis is to find the

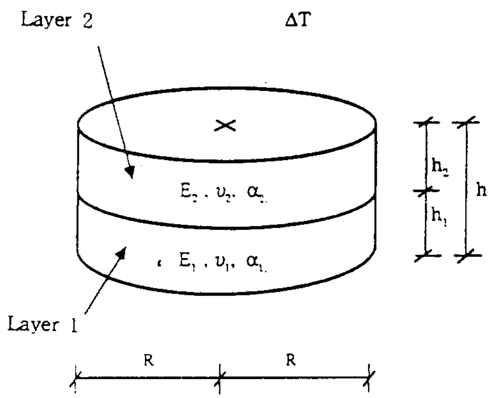

Figure 1. Configuration of the Bimaterial Disk

state of stress in the bimaterial disk subject to uniform temperature change with the condition that the lateral and radial surfaces of the disk remain traction-free. A two-step solution process will be undertaken for this problem. The first is in effect a "strength of materials" solution which is only approximate in that the only the resultant tractions are zero on the radial surface(r=R) of the disk, and not the tractions themselves. Next, a solution consistent with the linear theory of elasticity is formulated that depends crucially on knowledge of the strength of materials solution. This solution is formulated in terms of complex stress functions(Love) and results in an eigenvalues problem when continuity of traction and displacement across the interface is enforced. Stresses at points of interest within the disk must then be calculated by evaluating a finite series expansion.

3. Solution Method

3.1 Strength-Of-Materials Solution

The strength of materials solution is carried out assuming that the layers(disks) are thin in comparison to their radius. Let α_1 and α_2 denote the linear coefficients of thermal expansion of the two layers, E_1 and E_2 the moduli of elasticity, υ_1 and υ_2 the Poisson's ratios, h_1 and h_2 the layer thicknesses. The total thickness of the bi-material structure is denoted by h.

Figure 2 shows the cylindrical coordinates r, z_1 and z_2 associated with each layer.

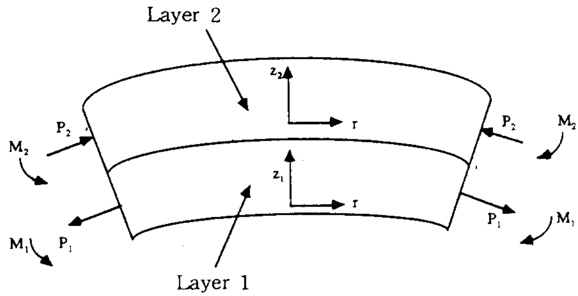

Figure 2. Forces and Moments Acting on Outer Radial Plane of the Bimaterial Disk

If $\alpha_2 > \alpha_1$, the deflection will be concave downward. All the tractions acting on the radial surface r=R of the layer 1 can be represented by a resultant tensile radial force P_1 and resultant bending moment M_1. Both P_1 and M_1 are measured per unit circumferential length. For layer 2 all tractions acting on the radial plane can be represented by a resultant compressive radial force P_2 and resultant bending moment M_2. Due to the fact that the resultant radial force and moment at r=R must vanish for the composite structure, the following conditions result.

$$P_1 = P_2 = P \tag{1}$$

$$\frac{Ph}{2} = M_1 + M_2 \tag{2}$$

If the interaction between the radial forces and moments is neglected, each disk will deform so as to maintain a constant radius of curvature ρ. For compatible deformation, the curvatures of each of the disks must be identical. The relationships between the bending moments and the radius of curvature is (Timoshenko, 1959)

$$M_1 = \frac{D_1(1+\upsilon_1)}{\rho} \quad (3)$$

$$M_2 = \frac{D_2(1+\upsilon_2)}{\rho} \quad (4)$$

where

$$D_\ell = \frac{E_\ell h_\ell^3}{12(1-\upsilon_\ell^2)} \quad (\ell=1,2) \quad (5)$$

The parameters D_1 and D_2 are often referred to as the flexural rigidities. Substituting (3) and (4) into (2) gives,

$$\frac{Ph}{2} = \frac{D_1(1+\upsilon_1)+D_2(1+\upsilon_2)}{\rho} \quad (6)$$

and yields,

$$P = \frac{2}{\rho h}\left(\frac{E_1}{1-\upsilon_1}\frac{h_1^3}{12}+\frac{E_2}{1-\upsilon_2}\frac{h_2^3}{12}\right) \quad (7)$$

On the interface, the radial strains in each layer must be equal. The radial strain has resulted from free thermal expansion, strain due to the radial force P, strain due to the curvature ρ. Thus,

$$\alpha_1\Delta T+\frac{1-\upsilon_1}{E_1}\frac{P}{h_1}+\frac{h_1}{2\rho}=\alpha_2\Delta T-\frac{1-\upsilon_2}{E_2}\frac{P}{h_2}+\frac{h_2}{2\rho} \quad (8)$$

Combining (7) and (8) yields

$$P=\frac{(\alpha_2-\alpha_1)\Delta T}{\frac{1}{E_1'A_1}+\frac{1}{E_2'A_2}+\frac{h^2}{4(E_1'I_1+E_2'I_2)}} \quad (9)$$

$$M_1=\frac{(\alpha_2-\alpha_1)\Delta T}{2\left(\frac{1}{E_1'A_1}+\frac{1}{E_2'A_2}+\frac{h^2}{4(E_1'I_1+E_2'I_2)}\right)}\frac{hE_2'I_2}{(E_1'I_1+E_2'I_2)} \quad (10)$$

$$M_2=\frac{(\alpha_2-\alpha_1)\Delta T}{2\left(\frac{1}{E_1'A_1}+\frac{1}{E_2'A_2}+\frac{h^2}{4(E_1'I_1+E_2'I_2)}\right)}\frac{hE_2'I_2}{(E_1'I_1+E_2'I_2)} \quad (11)$$

where

$$E_\ell'=\frac{E_\ell}{1-\upsilon_\ell} \quad A_\ell=h_\ell \quad I_\ell=\frac{h_\ell^3}{12} \quad (12)$$

After introducing the dimensionless ratios,

$$m=\frac{h_1}{h_2} \quad n=\frac{E_1'}{E_2'} \quad (13)$$

It can be shown that

$$P=\frac{E_2'h_2^2(m^3n+1)}{6(1+m)\rho} \quad (14)$$

$$M_1=\frac{E_2'h_2^3m^3n}{12\rho} \quad (15)$$

$$M_2=\frac{E_2'h_2^3}{12\rho} \quad (16)$$

$$\frac{1}{\rho}=\frac{6(1+m)(\alpha_2-\alpha_1)\Delta T}{h_2[3(1+m)^2+(1+mn)(m^2+\frac{1}{mn})]} \quad (17)$$

The stress in each layer can then be determined using the formulas

$$\sigma_{rr1}=\sigma_{\theta\theta 1}=\frac{E_1'}{\rho}z_1+\frac{P}{h_1} \quad (18)$$

$$\sigma_{rr2}=\sigma_{\theta\theta 2}=\frac{E_2'}{\rho}z_2-\frac{P}{h_2} \quad (19)$$

$$\sigma_{rz1}=\sigma_{rz2}=\sigma_{zz1}=\sigma_{zz2}=0 \quad (20)$$

Substituting (14) through (17) into (18) and (19), the following result is obtained.

Layer 1 :

$$\frac{\sigma_{rr1}}{(\alpha_2-\alpha_1)\Delta T\sqrt{E_1'E_2'}}=\frac{3mn(1+m)\frac{2z_1}{h_1}+\frac{m^3n+1}{m}}{[3(1+m)^2+(1+mn)(m^2+\frac{1}{mn})]\sqrt{n}} \quad (21)$$

$$\sigma_{\theta\theta 1}=\sigma_{rr1} \tag{22}$$

$$\sigma_{rz1}=0 \tag{23}$$

$$\sigma_{zz1}=0 \tag{24}$$

Layer 2 :

$$\frac{\sigma_{rr2}}{(\alpha_2-\alpha_1)\Delta T\sqrt{E_1'E_2'}}=\frac{3(1+m)\frac{2z_2}{h_2}-(m^3n+1)}{[3(1+m)^2+(1+mn)(m^2+\frac{1}{mn})]\sqrt{n}} \tag{25}$$

$$\sigma_{\theta\theta 2}=\sigma_{rr2} \tag{26}$$

$$\sigma_{rz2}=0 \tag{27}$$

$$\sigma_{zz2}=0 \tag{28}$$

The solution presented above is for the case of non-zero tractions of($\sigma_{rr}(R, z)$).

Since the resultant tractions are zero, an exact solution obeying the equations of elasticity and satisfying traction-free boundary conditions can be obtained if the solution described above(strength of material solution) is superposed with another solution for the case of Fig. 3c. The additional problem shown in Fig. 3c is not a thermal stress problem. Here, the tractions equal and opposite to those calculated in the strength of materials solution must be applied to the radial edge of a bimaterial disk with the same dimensions and material properties as described in the problem above. To follow are formulation and solution of this problem.

The problem which are solved next is depicted in Fig. 4. The geometry and material properties are the same as that discussed above. The loading on the radial plane r=R is the negative of the radial stresses computed according to the strength of materials theory. The self-equilibrating traction distribution is then

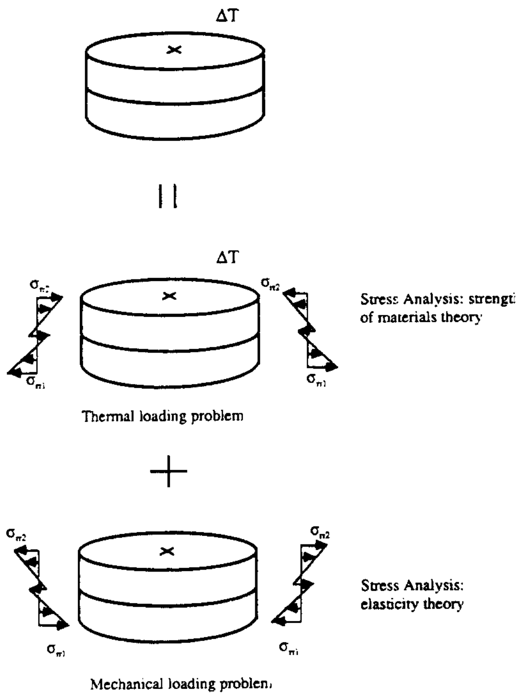

Figure 3. Superposition of Stress States

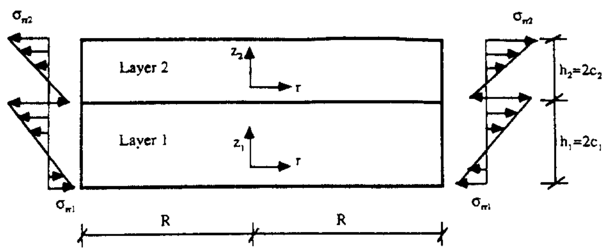

Figure 4. Bimaterial Disk with Applied Self-Equilibrating Stress Distribution

$$\frac{\sigma_{rr1}}{(\alpha_2-\alpha_1)\Delta T\sqrt{E_1'E_2'}}=-\frac{3mn(1+m)\frac{2z_1}{h_1}+\frac{m^3n+1}{m}}{[3(1+m)^2+(1+mn)(m^2+\frac{1}{mn})]\sqrt{n}}$$

$$|z_1|\le\frac{h_1}{2} \tag{51}$$

$$\sigma_{zz1}=\sigma_{rz1}=0, \qquad \sigma_{\theta\theta 1}=\sigma_{rr1} \tag{52}$$

$$\frac{\sigma_{rr2}}{(\alpha_2-\alpha_1)\Delta T\sqrt{E_1'E_2'}}= -\frac{3(1+m)\frac{2z_2}{h_2}-(m^3n+1)}{[3(1+m)^2+(1+mn)(m^2+\frac{1}{mn})]\sqrt{n}}$$

$$|z_2|\le\frac{h_2}{2} \qquad (53)$$

$$\sigma_{zz2}=\sigma_{rz2}=0, \qquad \sigma_{\theta\theta2}=\sigma_{rr2} \qquad (54)$$

3.2 Theory of Elasticity Solution

3.2.1 Eigenfunction Expansion Technique for Homogeneous Disk

For clarity, the formulation appropriate to a homogeneous disk of thickness h=2c will be presented prior to the formulation for the bi-material disk(see Fig. 5).

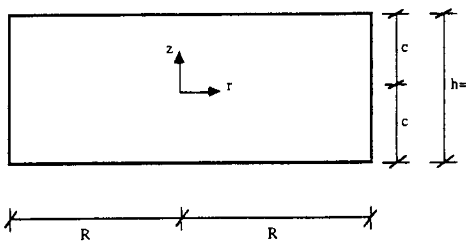

Figure 5. Homogeneous Disk

This problem is formulated using the Love stress function φ for axisymmetric elesticity (see Love[1927]). The Love stress function satisfies the biharmonic equation

$$\nabla^2\nabla^2\varphi=0 \qquad (55)$$

where

$$\nabla^2=\frac{\partial^2}{\partial r^2}+\frac{1}{r}\frac{\partial}{\partial r}+\frac{\partial^2}{\partial z^2} \qquad (56)$$

A solution to Eq.(55) in the form

$$\varphi(r,z)=I_0(\gamma\frac{r}{c})f(z) \qquad (57)$$

is sought, where I_0 is the modified Bessel function of the first kind of order zero, γ is a complex number, and f(z) is an as yet undetermined function. The following formulas regarding derivatives of the Bessel functions I_0 and I_1, are useful in the subsequent analysis. The modified Bessel function of first kind of order one is indicated by I_1.

$$\frac{d}{dr}I_0(wr)=w\,I_1(wr)$$

$$\frac{d}{dr}I_1(wr)=w\,I_0(wr)-\frac{1}{r}I_1(wr) \qquad (58)$$

When Eq.(57) is substituted into Eq.(55), an ordinary differential equation for f(z) can readily be expressed as

$$f(z)=(\frac{c}{\gamma})^3[(a_1+a_2\gamma\frac{z}{c})\cos\gamma\frac{z}{c}+(a_3+a_4\gamma\frac{r}{c}) \sin\gamma\frac{z}{c}] \qquad (59)$$

where a_1, a_2, a_3, and a_4 are as yet undetermined complex constants. Then the Love stress function and the associated stresses and strains are given by

$$\varphi(r,z)=(\frac{c}{\gamma})^3 I_0(\gamma\frac{r}{c})[(a_1+a_2\gamma\frac{z}{c}) \cos\gamma\frac{z}{c}+(a_3+a_4\gamma\frac{r}{c})\sin\gamma\frac{z}{c}] \qquad (60)$$

$$\sigma_{rr}=\frac{\partial}{\partial z}[\nu\nabla^2\varphi-\frac{\partial^2\varphi}{\partial r^2}]$$
$$=I_0(\gamma\frac{r}{c})[(-1-2\nu)a_2-a_3-a_4\gamma\frac{z}{c})\cos\gamma\frac{z}{c} -((1+2\nu)a_4-a_1-a_2\gamma\frac{z}{c})\sin\gamma\frac{z}{c}]$$
$$+\frac{I_1(\gamma\frac{r}{c})}{\gamma\frac{r}{c}}[(a_2+a_3+a_4\gamma\frac{z}{c})\cos\gamma\frac{z}{c} -(a_1-a_4+a_2\gamma\frac{z}{c})\sin\gamma\frac{z}{c}] \qquad (61)$$

$$\sigma_{\theta\theta}=\frac{\partial}{\partial z}(\nu\nabla^2\varphi-\frac{1}{r}\frac{\partial\varphi}{\partial r})$$
$$=-2\nu I_0(\gamma\frac{r}{c})(a_2\cos\gamma\frac{z}{c}+a_4\sin\gamma\frac{z}{c})$$

$$-\frac{I_1(\gamma\frac{r}{c})}{\gamma\frac{r}{c}}[(a_2+a_3+a_4\gamma\frac{z}{c})\cos\gamma\frac{z}{c}$$

$$-(a_1-a_4+a_2\gamma\frac{z}{c})\sin\gamma\frac{z}{c}] \qquad (62)$$

$$\sigma_{zz}=\frac{\partial}{\partial z}[(2-\nu)\nabla^2\varphi-\frac{\partial^2\varphi}{\partial z^2}]$$

$$=I_0(\gamma\frac{r}{c})[((-1+2\nu)a_2+a_3+a_4\gamma\frac{z}{c})\cos\gamma\frac{z}{c}$$

$$-((1-2\nu)a_4+a_1+a_2\gamma\frac{z}{c})\sin\gamma\frac{z}{c}] \qquad (63)$$

$$\sigma_{rz}=\frac{\partial}{\partial z}[(1-\nu)\nabla^2\varphi-\frac{\partial^2\varphi}{\partial z^2}]$$

$$=I_1(\gamma\frac{r}{c})[(-2\nu a_4+a_1+a_2\gamma\frac{z}{c})\cos\gamma\frac{z}{c}$$

$$+(2\nu a_2+a_3+a_4\gamma\frac{z}{c})\sin\gamma\frac{z}{c}] \qquad (64)$$

The corresponding radial displacement u_r and axial displacement w are given by

$$Eu_r=-(1+\nu)\frac{\partial^2\varphi}{\partial r\,\partial z}$$

$$=-(1+\nu)\frac{I_0(\gamma\frac{z}{c})}{\frac{\gamma}{c}}[(a_2+a_3+a_4\gamma\frac{z}{c})$$

$$\cos\gamma\frac{z}{c}-(a_1-a_4+a_2\gamma\frac{z}{c})\sin\gamma\frac{z}{c}] \qquad (65)$$

$$Ew=(1+\nu)[2(1-\nu)\nabla^2\varphi-\frac{\partial^2\varphi}{\partial r^2}$$

$$=(1+\nu)\frac{I_0(\gamma\frac{r}{c})}{\frac{\gamma}{c}}[(2(1-2\nu)a_4+a_1+a_2\gamma\frac{z}{c})]$$

$$\cos\gamma\frac{z}{c}+(-2(1-2\nu)a_2+a_3+a_4\gamma\frac{z}{c})\sin\gamma\frac{z}{c}] \qquad (66)$$

On the lateral surfaces of the disk the traction varies with r.

On z = −c

$$\sigma_{zz}=(r,-c)=AI\,(\gamma\frac{r}{c}) \qquad (67)$$

$$\sigma_{rz}=(r,-c)=CI_1(\gamma\frac{r}{c}) \qquad (68)$$

On z = +c

$$\sigma_{zz}(r,c)=BI_0(\gamma\frac{r}{c}) \qquad (69)$$

$$\sigma_{rz}(r,c)=DI_1(\gamma\frac{r}{c}) \qquad (70)$$

where A, B, C, D are constants. Substituting (61)-(64)into (67)-(70), the constants a_1, a_2, a_3, and a_4 are evaluated in terms of γ, giving

$$a_1=\frac{(A-B)(2\nu\cos\gamma-\gamma\sin\gamma)+(C+D)((1-2\nu)\sin\gamma-\gamma\cos\gamma)}{\sin2\gamma-2\gamma} \qquad (71)$$

$$a_2=\frac{-(A+B)\sin\gamma-(C-D)\cos\gamma}{\sin2\gamma+2\gamma} \qquad (72)$$

$$a_3=\frac{(A+B)(2\nu\sin\gamma+\gamma\cos\gamma)+(C-D)((2\nu-1)\cos\gamma-\gamma\sin\gamma)}{\sin2\gamma+2\gamma} \qquad (73)$$

$$a_4=\frac{(A-B)\cos\gamma-(C+D)\sin\gamma}{\sin2\gamma-2\gamma} \qquad (74)$$

3.2.2 Eigenfunction Expansion Technique for Bi-Material Disk

The results above can now be applied to solve the bi-material disk problem shown in Fig. 4. The bi-material disk is assumed to be formed by creating a perfect bond between two homogeneous disks of arbitrary thickness and elastic moduli. If this disk is loaded only at its outer radius (on top and bottom lateral surfaces free of traction), then an eigenvalue equation is obtained. Quantities pertaining to layer 1 and layer 2 will be denoted by the subscripts 1 and 2, respectively. For a perfect bond between the two layers, traction and displacement must be continuous across the interface. Thus,

$$[\sigma_{zz1},\ \sigma_{rz1}]_{z1=+c_1}=[\sigma_{zz2},\ \sigma_{rz2}]_{z2=-c_2} \qquad (75)$$

$$[u_{r1},\ w_1]_{z1=+c_1}=[u_{r2},\ w_2]_{z2=-c_2} \qquad (76)$$

Enforcing continuity of traction yields,

$$\frac{\gamma_1}{c_1}=\frac{\gamma_1}{c_2} \qquad (77)$$

$$A_2 = B_1, \quad C_2 = D_1 \tag{78}$$

Eq. (77) provides the relationship that must exist between γ_1 and γ_2 in order to ensure continuous tractions across the interface. If the disk is free of traction on its lateral surfaces ($z_1 = -c_1$, $z_2 = +c_2$), then $A_1=C_1=B_2=D_2=0$. Then enforcing continuity of displacements on the interface gives two homogeneous equation for B_1 and D_1.

$$B_1\left(\beta_1 - E'\beta_2 + \frac{8\gamma_1^2}{d_1} - E'\frac{8\gamma_2^2}{d_2}\right) - D_1\left(\frac{\sin 4\gamma_1 - 4\gamma_1}{d_1} + E'\frac{\sin 4\gamma_2 - 4\gamma_2}{d_2}\right) = 0 \tag{79}$$

$$B_1\left(\frac{\sin 4\gamma_1 + 4\gamma_1}{d_1} + E'\frac{\sin 4\gamma_2 + 4\gamma_2}{d_2}\right) + D_1\left(\beta_1 - E'\beta_2 + \frac{8\gamma_1^2}{d_1} - E'\frac{8\gamma_2^2}{d_2}\right) = 0 \tag{80}$$

where

$$E' = \frac{E_1}{E_2}\frac{\alpha_2}{\alpha_1} \tag{81}$$

$$\beta_\ell = \frac{1-2\nu_\ell}{1-\nu} \tag{82}$$

$$d_\ell = \sin^2 2\gamma_\ell - (2\gamma_\ell)^2 \tag{83}$$

$$\alpha_\ell = 1 - v_\ell^2 \quad (\ell = 1, 2) \tag{84}$$

Nontrivial solutions for B_1 and D_1 exist only for those values of γ_1 and γ_2 for which the determinant of the coefficient matrix in Eq. (79) and (80) vanishes, i.e.

$$\left(\frac{\sin 4\gamma_1 + 4\gamma_1}{d_1} + E'\frac{\sin 4\gamma_2 + 4\gamma_2}{d_2}\right)\left(\frac{\sin 4\gamma_1 - 4\gamma_1}{d_1} + E'\frac{\sin 4\gamma_2 - 4\gamma_2}{d_2}\right) + \left(\beta_1 - E'\beta_2 + \frac{8\gamma_1^2}{d_1} - E'\frac{8\gamma_2^2}{d_2}\right)^2 = 0 \tag{85}$$

This is the eigenvalue equation, a transcendental equation for γ_1 and γ_2. Roots of Eq.(85) are the values of γ_1 and γ_2 for which a solution of the end problem for the bi-material disk exists in the assumed form. The roots of Eq. (85) can be determined numerically. This is accomplished most conveniently by elimination γ_2 with Eq.(77). Solving this equation leads to a series of eigenvalues (γ_1^1, γ_2^1), ··· , (γ_1^i, γ_2^i), ··· , (γ_1^N, γ_2^N), where the superscript i indicate the i-th eigenvalue and the superscript N indicates the last eigenvalue computed. While there is an infinity of eigenvalues, only a finite number of them need to be computed for purpose of stress computation.

3.3 Satisfaction of End Tractions via Least Square Method

Once the eigenvalues have been obtained for a given set of physical and material parameters, it remains to compute the associated eigenfunctions and to combine them in a manner such that they satisfy the boundary conditions at the outer radius r=R. It is important to note that separate eigenfunctions exist for each layer, i.e. one function in layer 1(with $\gamma=\gamma_1$) and another in layer 2(with $\gamma=\gamma_2$). In this discussion, both functions are implied with the single term ***eigenfunction***. The stresses in each disk, due to the radial tractions alone, are given by Eq.(61-64) with the following values of a_{11}^i, a_{12}^i, a_{13}^i, and a_{14}^i. These values can be determined within a multiplicative complex constant C^i as follows ;

layer 1 : $A_1=C_1=0$, $\gamma=\gamma_1$

$$a_{11} = C\,\frac{-D(2\nu_1\cos\gamma_1 - \gamma_1\sin\gamma_1) + (1-2\nu_1)\sin\gamma_1 - \gamma_1\cos\gamma_1}{\sin 2\gamma_1 - 2\gamma_1} \tag{86}$$

$$a_{12}=C\frac{-D\sin\gamma_1+\cos\gamma_1}{\sin2\gamma_1+2\gamma_1} \tag{87}$$

$$a_{13}=C\frac{D(2\nu_1\sin\gamma_1+\gamma_1\cos\gamma_1)+(1-2\nu_1)\cos\gamma_1+\gamma_1\sin\gamma_1}{\sin2\gamma_1+2\gamma_1} \tag{88}$$

$$a_{14}=C\frac{-D\cos\gamma_1-\sin\gamma_1}{\sin2\gamma_1-2\gamma_1} \tag{89}$$

layer 2 : $B_2=D_2=0$, $A_2=B_1$, $C_2=D_1$, $\gamma=\gamma_2$

$$a_{21}=C\frac{D(2\nu_2\cos\gamma_2-\gamma_2\sin\gamma_2)+(1-2\nu_2)\sin\gamma_2-\gamma_2\cos\gamma_2}{\sin2\gamma_2-2\gamma_2} \tag{90}$$

$$a_{22}=C\frac{-D\sin\gamma_2-\cos\gamma_2}{\sin2\gamma_2+2\gamma_2} \tag{91}$$

$$a_{23}=C\frac{D(2\nu_2\sin\gamma_2+\gamma_2\cos\gamma_2)-(1-2\nu_2)\cos\gamma_2-\gamma_2\sin\gamma_2}{\sin2\gamma_2+2\gamma_2} \tag{92}$$

$$a_{24}=C\frac{D\cos\gamma_2-\sin\gamma_2}{\sin2\gamma_2-2\gamma_2} \tag{93}$$

where

$$D=\frac{d_2(\sin 4\gamma_1-4\gamma_1)+E'd_2(\sin4\gamma_2-4\gamma_2)}{d_1d_2(\beta_1-E'\beta_2)+8(d_2\gamma_1^2-E'd_1\gamma_2^2)} \tag{94}$$

In these equations, the right superscript i has been omitted to simplify the notation. The reader should be aware that it would appear on the left hand side of Eq.(86)-(94) and on the symbols γ_1, γ_2, C and D. Given N roots of Eq.(85), N eigenfunctions may be calculated, each with an arbirtrary coefficient C^i. Thus there are 2N real coefficients to be evaluated-the real and imaginary parts of C^i. These must now be selected so that the series. Expansion of the eigenfunctions will satisfy prescribed radial traction boundary conditions on the ends. Then a solution to the complete boundary value problem will have been obtained for the self-equilibrating end loading of Fig. 3c.

In order to proceed with the task of satisfying the end conditions, either the real or the imaginary part of the complex solution will be isolated. The choice in a matter of indifference since both satisfy the differential equations and homogeneous boundary conditions. The real part was selected for this analysis.

In general, it will not be possible to satisfy the boundary conditions exactly using only a finite number of terms in the series expansion, and the 2N real coefficients should be determined so as to minimize the error incurred in truncating the series. A well-known technique is the method of *least squares*, which provides the best fit of the eigenfunction series to the end conditions at each of a finite number of points on the ends. If M points are selected on each end, with $M\geq N$, then the least squares procedure will result in values of the coefficients C^i that minimize the mean square error of the solution at the selected points. The procedure follows. The radial and shear stress in each layer are written as a sum of the product of coefficients C^i and eigenfunctions $f_r(\gamma^i_\ell)$, $f_s(\gamma^i_\ell)$ as

$$\sigma_{rr}=\mathrm{Re}\left(\sum_{i=1}^{N} C^i f_r(\gamma^i_\ell)\right) \tag{95}$$

$$\sigma_{rz}=\mathrm{Re}\left(\sum_{i=1}^{N} C^i f_s(\gamma^i_\ell)\right) \tag{96}$$

where

$$f_r(\gamma^i_\ell)=I_o\left(\gamma^i_\ell\frac{r}{c_\ell}\right)\left[\left(-1-2\nu_\ell\right)a^i_{\ell2}-a^i_{\ell3}-a^i_{\ell4}\gamma^i_\ell\frac{z_\ell}{c_\ell}\right)$$

$$\cos\gamma^i_\ell \frac{z_\ell}{c_\ell} - \left((1+2\nu_\ell a^i_{\ell 4} - a^i_{\ell 1} - a^i_{\ell 2}\gamma^i_\ell \frac{z_\ell}{c_\ell}\right) \sin\gamma^i_\ell \frac{z_\ell}{c_\ell} \Big] + \frac{I_1(\gamma^i_\ell \frac{r}{c_\ell})}{\gamma^i_\ell \frac{r}{c_\ell}}$$

$$\Big[(a^i_{\ell 2} + a^i_{\ell 3} + a^i_{\ell 4}\gamma^i_\ell \frac{z_\ell}{c_\ell})\cos\gamma^i_\ell \frac{z_\ell}{c_\ell} - (a^i_{\ell 1} - a^i_{\ell 4} + a^i_{\ell 2}\gamma^i_\ell \frac{z_\ell}{c_\ell})\sin\gamma^i_\ell \frac{z_\ell}{c_\ell}\Big] \tag{97}$$

$$f_s(\gamma^i_\ell) = I_1(\gamma^i_\ell \frac{r}{c_\ell})\Big[(-2\nu_\ell a^i_{\ell 4} + a^i_{\ell 1} + a^i_{\ell 2}\gamma^i_\ell \frac{z_\ell}{c_\ell})\cos\gamma^i_\ell \frac{z_\ell}{c_\ell} + (2\nu_\ell a^i_{\ell 2} + a^i_{\ell 3} + a^i_{\ell 4}\gamma^i_\ell \frac{z_\ell}{c_\ell})\sin\gamma^i_\ell \frac{z_\ell}{c_\ell}\Big] \tag{98}$$

where $\ell=1, 2$(layer number), $i=1, \cdots, N$(i-th eigenvalue).

In these equations it should be noted that $a^i_{\ell 1}-a^i_{\ell 4}$ are as given by Eq.(86)-(94), with the coefficient C^i deleted. The real and imaginary parts of C^i, f_r and f_s are separated according to

$$C^i = x_i + iy_i \tag{100}$$

$$f_r(\gamma^i_\ell) = \text{Re } f_r(\gamma^i_\ell) + i\ \text{Im}f_r(\gamma^i_\ell) \tag{101}$$

$$f_s(\gamma^i_\ell) = \text{Re } f_s(\gamma^i_\ell) + i\ \text{Im}f_s(\gamma^i_\ell) \tag{102}$$

where $i=\sqrt{-1}$

$$\sigma_{rr\ell} = x_1\text{Re}f_r(\gamma^1_\ell) + x_2\text{Re}f_r(\gamma^2_\ell)\cdots + x_N\text{Re}f_r(\gamma^N_\ell) - y_1\text{Im}f_r(\gamma^1_\ell) - y_2\text{Im}f_r(\gamma^2_\ell) - \cdots - y_N\text{Im}f_r(\gamma^N_\ell) \tag{103}$$

$$\sigma_{rz\ell} = x_1\text{Re}f_s(\gamma^1_\ell) + x_2\text{Re}f_s(\gamma^2_\ell)\cdots + x_N\text{Re}f_s(\gamma^N_\ell) - y_1\text{Im}f_s(\gamma^1_\ell) - y_2\text{Im}f_s(\gamma^2_\ell) - \cdots - y_N\text{Im}f_s(\gamma^N_\ell) \tag{104}$$

The mean square error E for the tractions on the outer radial edge r=R can be written,

$$E = \sum_{k=1}^{M}[(\sigma_{rr}(R, z_{\ell k}) - R_k)^2 + (\sigma_{rz}(R, z_{\ell k}) - S_k)^2] \tag{105}$$

where R_k, S_k are

$$R_k = -\Big[\frac{P}{A_1} + \frac{M_1 z_{1k}}{I_1}\Big] \quad -\frac{h_1}{2} \le z_{1k} \le \frac{h_1}{2} \tag{106}$$

$$R_k = -\Big[\frac{P}{A_2} + \frac{M_2 z_{2k}}{I_2}\Big] \quad -\frac{h_2}{2} \le z_{2k} \le \frac{h_2}{2} \tag{107}$$

$$S_k = 0, \quad -\frac{h_1}{2} \le z_{1k} \le \frac{h_1}{2}, \quad -\frac{h_2}{2} \le z_{2k} \le \frac{h_2}{2} \tag{108}$$

The symbol M is the number of the points where the tractions are specified on the end r=R. To minimize E, the coefficients x_i and y_i are chosen so that they satisfy the following conditions.

$$\frac{\partial E}{\partial x_1} = \cdots = \frac{\partial E}{\partial y_N} = 0 \tag{109}$$

Using these conditions yields a system of linear equations(2N) in the form of $A_x=b$ that can be solved for the constant x_i and y_i, where

A=[ ]
X=[ ] b=[ ]

where Σ denotes the summation of 1 to M.

Once the coefficient C^i are known, computing the stress at any point in the bi-material disk is a matter of evaluating the following finite series expansion.

$$\sigma_{rr1} = \frac{P}{A_1} + \frac{M_1 z_1}{I_1} + \text{Re}\Big(\sum_{i=1}^{N} C^i f_r(\gamma^i_1)\Big) \quad -\frac{h_1}{2} \le z_1 \le \frac{h_1}{2} \tag{110}$$

$$\sigma_{rr2} = -\frac{P}{A_2} + \frac{M_2 z_2}{I_2} + \text{Re}\Big(\sum_{i=1}^{N} C^i f_r(\gamma^i_2)\Big) \quad -\frac{h_2}{2} \le z_2 \le \frac{h_2}{2} \tag{111}$$

$$\sigma_{zz1}=\text{Re}\left(\sum_{i=1}^{N} C^i f_z(\gamma_1^i)\right) \quad -\frac{h_1}{2}\le z_1\le\frac{h_1}{2} \qquad (112)$$

$$\sigma_{zz2}=\text{Re}\left(\sum_{i=1}^{N} C^i f_z(\gamma_2^i)\right) \quad -\frac{h_2}{2}\le z_2\le\frac{h_2}{2} \qquad (113)$$

$$\sigma_{rz1}=\text{Re}\left(\sum_{i=1}^{N} C^i f_s(\gamma_1^i)\right) \quad -\frac{h_1}{2}\le z_1\le\frac{h_1}{2} \qquad (114)$$

$$\sigma_{rz2}=\text{Re}\left(\sum_{i=1}^{N} C^i f_s(\gamma_2^i)\right) \quad -\frac{h_2}{2}\le z_2\le\frac{h_2}{2} \qquad (115)$$

4. Numerical Results and Comparison with Finite Element Analysis

Physical properties for a molybdenum / aluminum bi-material disk were selected for a numerical example. The following physical data was used :

Aluminum

$E_1=70{,}380\text{MPa}(10.2\times10^6\text{psi})$ $\nu_1=0.345$

$\alpha_1=23.6\times10^{-6}\,{}^0\text{C}^{-1}$

Molybdenum

$E_2=325{,}000\text{MPa}(47.1\times10^6\text{psi})$ $\nu_2=0.293$

$\alpha_2=4.9\times10^{-6}\,{}^0\text{C}^{-1}$

$h_1=h_2=2.5\text{mm}(0.1\text{in})$ $h=5.0\text{mm}(0.2\text{in})$

$\Delta T=240^0\text{C}$.

Computations were performed for R/h ratios of 5, 2.5 and 1, representing a range from a relatively thin disk to a relatively thick one. In each plot to follow, stress is nondimensionalized by the factor $|\alpha_2-\alpha_1|\,\Delta T\sqrt{E_1'E_2'}$ with the dimensionless radial coordinate of r/R.

The distribution of radial stress σ_{rr} along the interface in the aluminum layer is shown Fig. 6. These results correspond to an eigenfunction series truncated to 25 terms with 101 points used for the least squares "fit" to satisfy the stress-free conditions at the radial edge of the disk. For the thin disk (R/h=5.0) the radial stress predicted by the eigenfunction series solution approaches the strength of materials(SOM) solution at a distance of approximately $h=h_1+h_2$ from each end, while for the thick disk(R/h=1.0), the actual stress(as predicted analytically) is not represented accurately by the SOM solution. The reader is reminded that the SOM solution predicts a uniform radial stress in each layer, and zero normal and shear stresses. The eigenfunction series solution is unable to satisfy the zero radial stress boundary condition at r=R due to the finite number of terms used in the least square fit. A subsequent finite element analysis(FEA) will show the degree to which the lack of satisfaction of this boundary condition effects the solution over the remaining radial dimension of the disk.

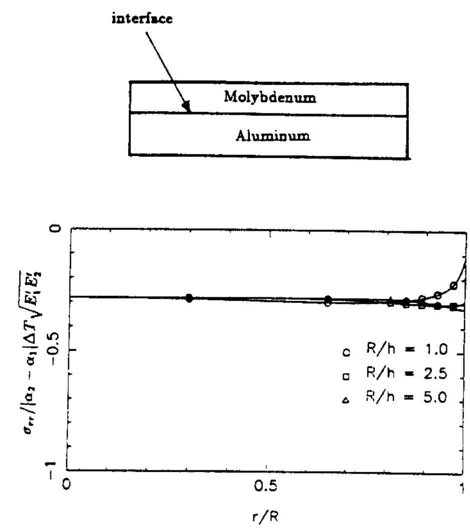

Figure 6. Distribution of Radial Stress σ_{rr} Along the Interface in Aluminum Layer

Upon examining the distribution of the computed shear σ_{rz} along the interfacem, shown in Fig. 7, it is clear that this stress component is essentially negligible for $0<\frac{r}{R}<0.8$, then rises rapidly before decaying to zero at the edge r=R. Again, the eigenfunction series does not satisfy the zero stress boundary condition at r=R. However, subsequent FEA results will show that the peak value of the shear stress is predicted very accurately with eigenfunction solution.

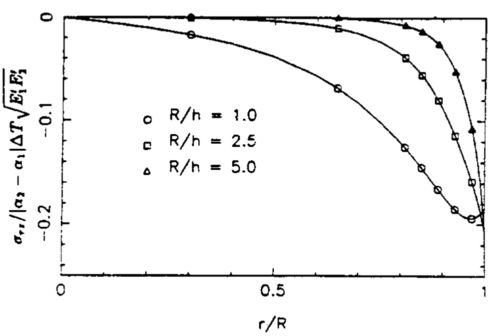

Figure 7. Distribution of Shear Stress σ_{rz} Along the Interface in Aluminum Layer

The distribution of normal stress σ_{zz} at the interface, shown in Fig. 8, changes sign rapidly near the edge r=R. This behavior is anticipated because static equilibrium requires zero resultant force in the z direction. The results shown in Fig. 8 indicate that the magnitude of the normal traction on the interface assumes a very large magnitude as $\frac{r}{R}\rightarrow 1$, and this is because the normal stress in truly singular at the edge r=R. The eigenfunction

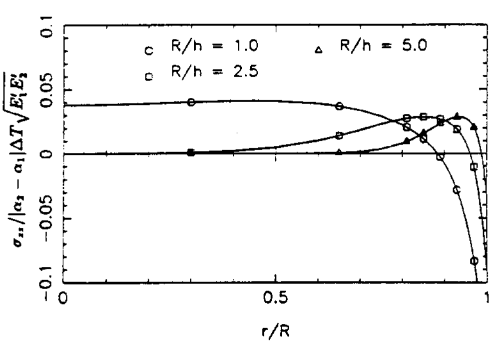

Figure 8. Distribution of Normal Stress σ_{zz} Along the Interface in Aluminum Layer

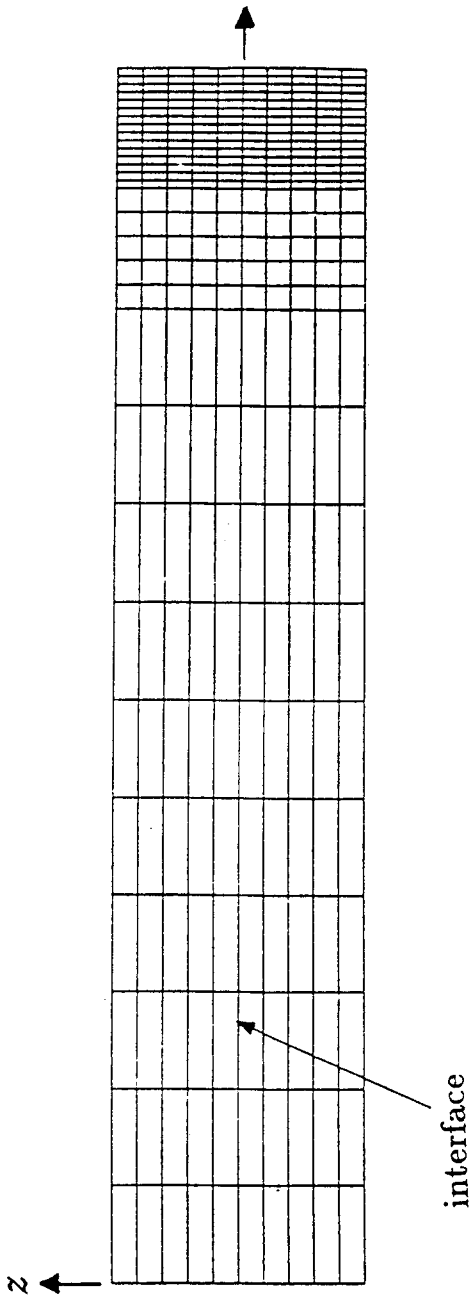

Figure 9. Finite Element Mesh Plot

series solution is unable to capture this behavior exactly. In light of this fact, it would be very difficult to obtain the degree of the singularity from this solution. However, this is not a significant drawback since the degree of the singularity is already known from independent elasticity analyses of bonded dissimilar material(see Bogy 1970).

The analytical results discussed above have been verified by independent Finite Element Analysis(FEA). To obtain a reasonably smooth stress distribution at the interface near the end, a fine mesh is required. Due to the absence of singular terms in the displacement interpolation functions of the finite elements, a very fine mesh, containing 981 nodes and 300 elements, were employed in this analysis. A mesh plot is shown in the Fig. 9. The results for the case R/h=2.5 will be presented. The radial stress σ_{rr} along the interface in the aluminum layer is shown in Fig. 10. The FEA solution comes much closer to the satisfying the stress-free boundary condition at r=R.

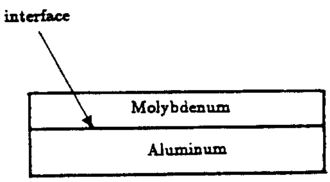

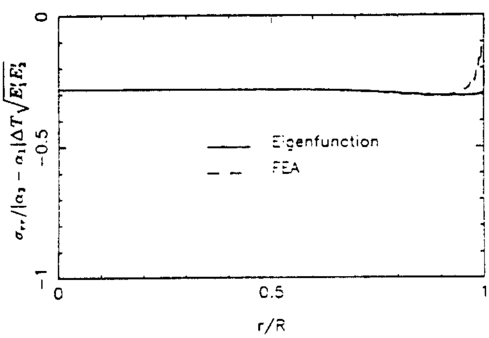

Figure 10. Comparison Eigenfunction/ FEA for Radial Stress σ_{rr}, R/ h=2.5

The distribution of shear stress σ_{rz} is shown in Fig. 11. It is clear that peak magnitude of the shear stress is in complete agreement with the eigenfunction and FEA solutions. Again, the FEA solution shows that the stress does decay over a very short interval near the edge r=R.

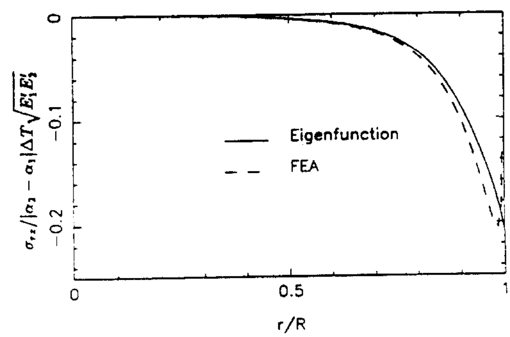

Figure 11. Comparison Eigenfunction/ FEA for ShearStress σ_{rz}, R/ h=2.5

Further mesh refinement leads to a distribution of stress which is very nearly zero at the edge. The normal(peeling) stress distribution is shown in Fig. 12. Again the eigenfunction and FEA solutions are generally in agreement. The FEA solution near the free edge has sharp peak, which may be result of the possible singular behavior, compared to eigenfuntion analysis.

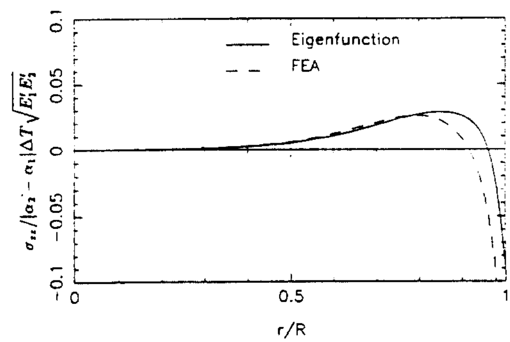

Figure 12. Comparison Eigenfunction/ FEA for Normal Stress σ_{zz}, R/ h=2.5

5. Conclusion

In conclusion, two independent methods of predicting the interfacial normal and shear stresses in a binaterial disk subjected to thermal loading have been developed. These are : 1) the solution following the strength of materials principle, 2) theory of elasticity solution via an eigenfunction expansion approach. The SOM solutions predict a uniform radial stress independent of radial position in each layer, and zero normal and shear stress. These SOM solutions have difficulty in predicting both the peak value of interfacial stresses and associated distribution. The theory of elasticity solutions are compared with finite element stress analysis results for a specific numerical example. Finite element analysis results show that the interfacial stresses are predicted adequately by eigenfunction solution. Therefore, the method developed in this paper will be useful in determination of the interfacial stress state.

References

1. Bogy, D. B., (1970), "On the Problem of Edge Bonded Elastic Quater-Planes Loaded at the Boundary," *International Journal of Solids and Structures*, Vol. 6, pp.1287-1313.
2. Churchill, R. V., and Brown, J. W.,(1984), Complex Variables and Applications, 4th Ed., pp.152, McGraw-Hill Book Company.
3. Hess, M. S., (1969), "The End Problem for a Laminated Elastic Strip-Ⅱ, Differential Expansion Stresses," *Journal of Composite Materials*, Vol. 3, pp.630-641.
4. Love, A. E. H., (1927), A Treatise on the Mathematical Theory of Elasticity, 4th ed., pp.274, Cambridge University Press, New York.
5. Suhir, E., (1986), "Stresses in Bi-Metal Thermostats," *Journal of Applied Mechanics, Trans.* ASME, Vol. 53, pp.657-660.
6. Suhir, E., (1988), "An Approximate Analysis of Stresses in Multilayeres Elastic Thin Films," *Journal of Applied Mechanics*, Vol. 55, pp. 143-148.
7. Suhir, E., (1989), "Interfacial Stresses in Bimetal Thermostats," *Journal of Applied Mechanics*, Vol. 56, No. 3, pp.595-600.
8. Timoshenko, S., (1925), "Analysis of Bi-Metal Thermostats," *Journal of the Optical Society of America*, Vol. 11, pp.233-255.
9. Timoshenko, S. P., (1959), Theory of Plates and Shells, pp.43, McGraw-Hill Book Company, Inc..
10. Timoshenko and Goodier, (1970), Theory of Elasticity, 3rd. Ed., pp.380-382, McGraw-Hill Book Company, Inc..
11. Vilms, J. and Kerps, D., (1982), "Simple Stress Formula for Multilayered Thin Films on a Thick Substrate," *Journal of Applied Physics*, Vol. 53, No. 3, pp.2-7.

(접수일자 : 1994. 12. 21)